

**Sound in a granular material: Disorder and nonlinearity**

Chu-heng Liu and Sidney R. Nagel

*The James Franck Institute and The Department of Physics, The University of Chicago,  
5640 South Ellis Avenue, Chicago, Illinois 60637*

(Received 16 April 1993; revised manuscript received 3 September 1993)

We have investigated the properties of low-amplitude vibrations in dry unconsolidated granular materials. The velocity of sound can vary by a factor of 5 depending upon whether one measures either the arrival time of the rising edge of the pulse or the quantity analogous to the group velocity. If we increase the amplitude of the vibrations, we observe nonlinearity near the point at which we first see hysteretic behavior. This is interpreted as due to the presence of force chains. We also find frequency shifts in all of the features that characterize the transmission spectrum.

Granular media have interesting features that distinguish them from other systems.<sup>1</sup> Nowhere is this more apparent than in the phenomenon of sound propagation. In the frequency regime where the wavelength is comparable to the granularity of the media, we have found<sup>2</sup> that the sound shows an extreme dependence on the position of each grain—so much so that even the tiny motions caused by the sound vibration itself (or by minute temperature fluctuations in the medium) can cause the amplitude of the detected signal to fluctuate with time. The power spectrum for the fluctuations caused by the vibrations themselves varied approximately as  $f^{-2}$  (Ref. 3). This implies that nonlinearity is particularly important in these unconsolidated media; the structure of the pile is determined by the fragile contacts between the grains so that even small vibrations will cause the structure to evolve in time and produce fluctuations in the transmitted sound amplitude. In addition, we have found a delicate but reproducible dependence of the transmission amplitude on the frequency of the source at low vibration amplitudes. Disorder is, therefore, also important since it gives rise to interference effects that can lead to conductance fluctuations (in frequency) or possibly even to localization of the waves. At low frequencies, where the wavelength of the sound is large compared to the granularity of the medium, we have argued that it may not be possible to have any horizontal sound propagation at all due to mirage effects which govern the trajectories of the sound and bend all paths towards the vertical direction. In this paper we will extend our previous studies to investigate further aspects of sound propagation in these unconsolidated systems. In particular, we will investigate the role of the source amplitude in order to study the effects of nonlinearity.

As in our previous experiments,<sup>2</sup> we used 0.5-cm-diam dry spherical glass beads contained in a square box of side 28 cm with a depth of 8 to 15 cm. The configuration is shown in Fig. 1(a). We reduced the reflection of the sound waves from the walls by lining the box with Styrofoam sheets. The box is isolated from external vibrations and temperature fluctuations by several other layers of Styrofoam sheets and enclosed in a plastic container filled with dry nitrogen gas. This last enclosure further stabi-

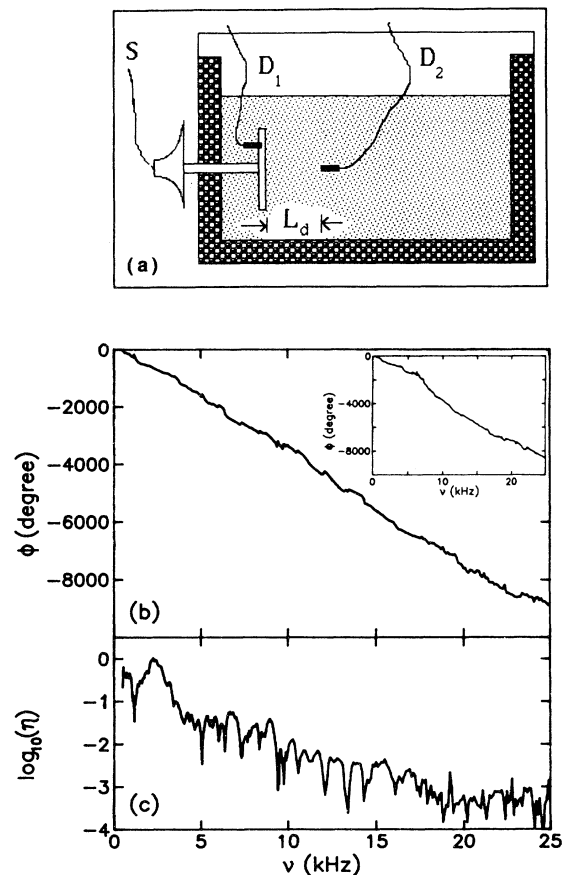


FIG. 1. (a) A schematic diagram of the side view of the experimental configuration.  $D_1$  and  $D_2$  correspond, respectively, to the two detectors used to monitor the source acceleration and the detected signal.  $S$  represents the source speaker. The walls are padded with 3-cm-thick sheets of Styrofoam. In (b) the phase  $\phi$  and in (c) the transmission  $\eta$  are shown as functions of the frequency  $\nu$  for a detector at distance  $L_d=6$  cm from the source. The slope of  $\phi(\nu)$  determines  $c_g$ . The inset to (b) shows the phase  $\phi$  for a different microscopic configuration of the beads. This is the curve of  $\phi(\nu)$  which is the least linear that we have found.

lizes the system against fluctuations in humidity. We connected a 7-cm-diam aluminum disk inside the box to an external speaker in order to transmit the vibrations with a well-defined direction of motion. The acceleration of the disk was monitored with an accelerometer (labeled  $D_1$  in the figure) attached to its back and controlled with an electronic feedback loop. The detection accelerometers (labeled  $D_2$ ) had a diameter of 0.7 cm and a length of 1.2 cm. They were comparable to the size of a single grain and placed at distances from 2 to 10 cm away from the center of the source. Because of their huge mass density compared to air, the accelerometers respond only to vibrations transmitted through their contacts with the solid surroundings instead of to the sound pressure in air. This has been confirmed by two means: (i) a (smaller) box of sand was evacuated and similar results were obtained; (ii) the transducer was submitted to vibrations carried only by air and no signal was seen.

The first question we address is what is the velocity of sound in this medium? As we mentioned above for low frequencies, even such a straightforward measurement can be problematic since there is presumably a large depth dependence to the velocity. There are at least two different experiments which we can use to determine this quantity. The first is the time-of-flight method where we create a pulse at the source and measure the time it takes for the first effect to be felt at the detector. This yields the value  $c_{\text{tof}} = 280 \pm 30$  m/s at a depth of 6 cm. This value is close to the velocity of sound in air so we checked that the velocity we measured was due only to the propagation through the sand by remeasuring the velocity in an evacuated box and one filled with helium gas ( $c = 970$  m/s). In both cases we found the same value for the sound speed. A second measurement can be used to measure a quantity analogous to the group velocity. To do this we measure the phase  $\phi$  of the detected signal at the detector as a function of frequency  $\nu$ . We can determine the group velocity  $c_g$  from the slope of  $\phi(\nu)$  and the distance  $L_d$  between the source and detector:  $c_g = 2\pi L_d d\nu/d\phi$ . In Fig 1(b) we show  $\phi(\nu)$  over the range  $500 \text{ Hz} < \nu < 25\,000 \text{ Hz}$  for the case where  $L_d = 6$  cm. To a good approximation, the phase in Fig. 1(b) varies linearly with frequency over the entire range of  $\nu$ . The fluctuations about this linear dependence are quite small. For this slope we calculate  $c_g = 57$  m/s, which is almost five times slower than that measured by the time-of-flight experiment. As the arrangement of the beads is changed, the slope of the  $\phi(\nu)$  also changes. Sometimes, even a linear fit is questionable. In the inset of Fig. 1(b), we show one curve which shows the largest deviation from a linear dependence which we have found. If we use the averaged slope  $d\phi/d\nu$ , the value of  $c_g$  can vary within a range of 50–90 m/s depending on the detailed grain configuration.

Although the phase appears to have a reasonably smooth frequency dependence, the amplitude of the detector does not. We show this in Fig. 1(c), where we plot the transmission  $\eta \equiv A_d/A_s$  versus frequency. In addition to the general trend of decreasing transmission with increasing  $\nu$ , we see very sharp and dramatic variations with frequency. These features correspond to the

small fluctuations about the linear behavior in the  $\phi(\nu)$  curve. As we have reported previously,<sup>2</sup> these sharp features are reproducible if the curve is retaken immediately. A slight disturbance can change the features in the frequency response curve in Fig. 1. This disturbance does not need to be close to the detector. A minute expansion of a bead (of about 1000 Å) located several centimeters away from the detector can generate a significant change. Although it is true that, on average, the signal depends more on the contacts which are closer to the detector, it is not true that a few contacts dominate the response. The spatial dependence is very irregular and provides another signature of the particular bead packing.<sup>4</sup>

The discrepancy between  $c_{\text{tof}}$  and  $c_g$  indicates complicated behavior in the propagation of the sound. In order to explore this in more detail, we have measured  $R(\tau)$ , the response to a  $\delta$ -function input as a function of elapsed time  $\tau$ . In principle, for a linear system this can be derived from a Fourier transform of the data in Fig. 1. Practically, however, higher accuracy can be obtained by measuring this function directly. We send a short pulse from the source and measure both the signal and the response with detectors  $D_1$  and  $D_2$ , respectively. Since we cannot make the pulse arbitrarily short due to ringing in the speaker, we must use the signals from both detectors in order to determine  $R(\tau)$ . We divide the suitably filtered Fourier transform of the signal from  $D_2$  by that from  $D_1$ . The inverse Fourier transform of this ratio is the response to a  $\delta$ -function input,  $R(\tau)$ . As one would expect for a linear system, this measured  $R(\tau)$  is fully consistent with the inverse Fourier transform of the frequency response data in Fig. 1 and shows that the results are not dependent on the frequency response or shifts of the speaker driving the source.

Data for  $R(\tau)$  are shown in Fig. 2 for the detector at four different distances from the source:  $L_d = 2, 4, 6,$  and  $8$  cm. We determine  $c_{\text{tof}}$  by measuring the onset of the first peak as a function of distance. Likewise, we can obtain the value of  $c_g$  by calculating the average slope of the phase as a function of frequency. Both values agree with what we obtained above so that we conclude that the discrepancy between the two values is not due to a nonlinear response in the medium.

In Fig. 2, we can see how the structure in  $R(\tau)$  develops with the distance  $L_d$  from the source to the detector. At small  $L_d$ , there is one dominant peak at short times followed by a number of smaller oscillations. As  $L_d$  increases, the first peak decreases and two structures of comparable height appear in the signal. It is tempting to think of the different peaks as corresponding to different paths via which the sound can travel. These paths then give rise to interference effects.

This interpretation of the sound propagation along a few discrete paths determined by the geometry of the contacts is quite distinct from the more conventional assumption that the sound behaves as a wave diffusing through a random medium.<sup>5</sup> The properties of such diffusing waves have been studied in a variety of contexts, including electron scattering in mesoscopic metals<sup>6</sup> and light propagation in a densely scattering medium.<sup>7</sup>

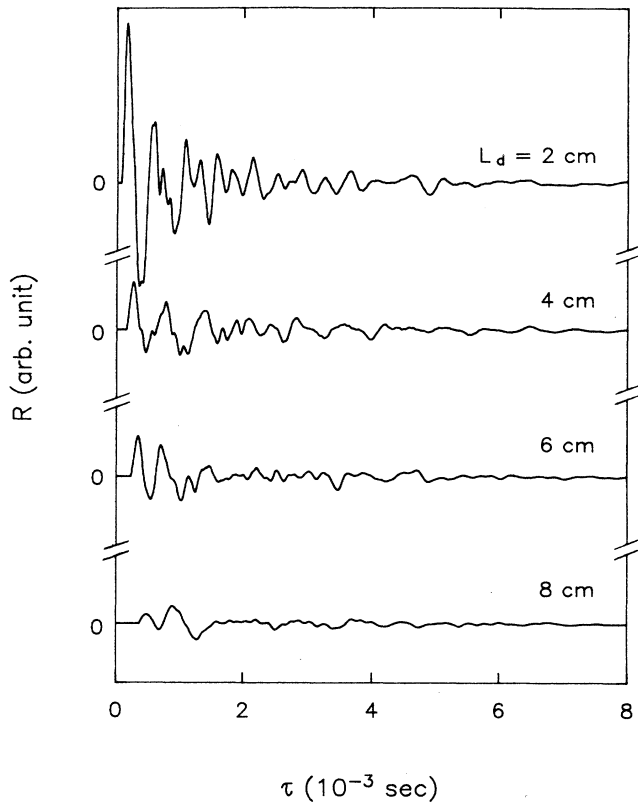


FIG. 2. The response function  $R$  as a function of elapsed time  $\tau$  for four different placements of the detector:  $L_d = 2, 4, 6,$  and  $8$  cm as labeled in the figure.

Sound in sand is different from these other cases since one suspects that there must be force chains, or arches, which span the distance between the source and detector.<sup>8</sup> These chains bear most of the burden for keeping the structure rigid. One might expect that, independent of frequency, all the sound waves must pass through the same set of force-bearing contacts. In this scenario it is not clear that the analysis used for describing electron or light diffusion can also be used to attack the problem of sound propagation in a granular medium. In Fig. 3(a), we plot the absolute value of the data,  $|R(\tau)|$ , of the curve from Fig. 2 for  $L_d = 4$  cm. After smoothing, we fit this data with a form appropriate to three-dimensional diffusion:<sup>9</sup>  $R(\tau) = A\tau^{-3/2}\exp(-B/\tau)$ , where  $A$  and  $B$  are constants. The diffusion form does look like a good envelope of the response-function data. In Fig. 3(b), we show  $\tau_{\max}$ , the time delay of the maximum of the diffusion fit versus the source-detector distance  $L_d$ . The diffusion wave picture naturally leads to a prediction that  $\tau_{\max}$  depends quadratically on the distance:  $\tau_{\max} \sim L_d^2$ . However, we see that the data follow a linear, not a quadratic form, which gives rise to a constant velocity  $dL_d/d\tau_{\max} = 110 \pm 15$  m/s. Unless we assume that the effective dimensionality of the diffusion paths changes with distance from the source, it is clear that the averaged response is inadequate to characterize the wave propagation in sand. We argue that the number of the

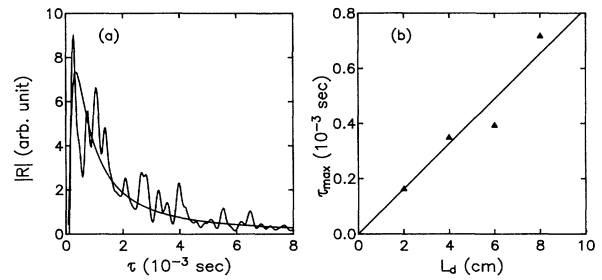


FIG. 3. (a) The absolute value of the response function  $|R(\tau)|$  at  $L_d = 4$  cm is smoothed and then fit with a form appropriate for diffusion:  $R(\tau) = A\tau^{-3/2}\exp(-B/\tau)$ . (b) The elapsed time of the maximum response  $\tau_{\max}$  as a function of source detector separation  $L_d$ .

preferred chains is so few that every individual peak is crucial to the final response. This interpretation is consistent with the importance of hysteretic effects since the force chains (arches) can break and reform in different patterns in the course of time, due to even small vibrations.

If we now vary the amplitude of the source signal  $A_s$ , we can investigate some of the nonlinear effects in this system. Figure 4 shows the amplitude of the detected wave  $A_d$  as a function of the source amplitude. At low amplitudes,  $A_d$  varies linearly with  $A_s$ . As  $A_s$  increases

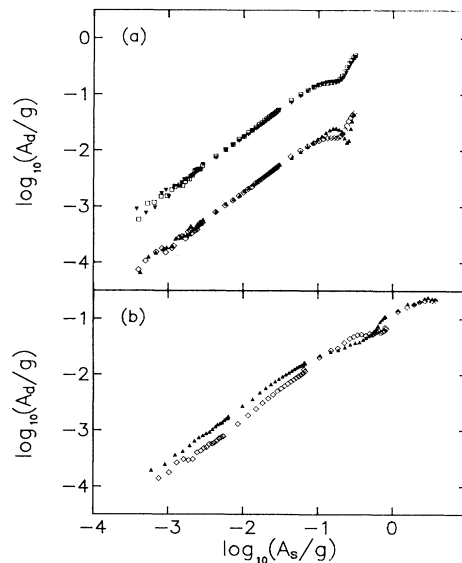


FIG. 4. The detector amplitude  $A_d$  vs the source amplitude  $A_s$ . Each set of curves corresponds to first increasing (filled symbols) and subsequent decreasing of  $A_s$  (open symbols). In (a) the lower curve shows the behavior during the first run at a given frequency of increasing and then decreasing  $A_s$ . Clear hysteresis is evident at large values of  $A_s$ . The upper curve, displaced vertically for clarity, shows what happens during subsequent runs where the hysteresis has almost completely disappeared. In (b) we show what happens when  $A_s$  is increased farther into the nonlinear regime. The hysteresis now occurs over the entire range of  $A_s$ .

above 0.1 g, we find that the behavior begins to depart from linearity. At about the same value of  $A_s$  we see that hysteresis becomes apparent; the curve measured when decreasing the amplitude (open symbols) does not reproduce the initial curve measured with  $A_s$  increasing (filled symbols). This indicates that there is movement of the particles so that the sound paths are altered. In the bottom set of curves in Fig. 4(a), where  $A_s$  is increased only slightly into the nonlinear regime, we see that the two traces taken by first raising and then lowering  $A_s$  are different from each other only at large values of  $A_s$ , whereas they seem to coincide at low amplitudes. If we now repeat the measurement a second time at the same frequency [as shown in the upper curves of Fig. 4(a)] we find that on increasing  $A_s$  we recover almost the identical curve that was last obtained on lowering  $A_s$ . Subsequent runs at this frequency continue to repeat this same behavior. Thus, most of the changes in the curve take place in the first run of increasing  $A_s$ . However, if we now change the source frequency, we again find strong hysteretic behavior during the first run and only after this do we get reproducible behavior at that frequency. In Fig. 4(b), we see that when  $A_s$  is increased even further, the two traces remain different over the entire span of  $A_s$ .

We hypothesize that when the amplitude has not been increased too much, the changes that occur in the pile are of two distinct kinds. At low amplitudes we see only linear and reproducible behavior which does not change even after increasing the source amplitude into the nonlinear regime. We believe the motions that occur in these runs are due to the grains not belonging to the primary force chains. At larger source amplitudes these small motions can change the sound propagation since the amplitude of oscillation is sufficient in this regime to bring into contact particles which had not previously been touching (consistent with the onset of nonlinear behavior near this point), whereas, at low amplitude they do not contribute to the sound propagation. Upon changing the source frequency a new region of the sample is affected since the maximum in the oscillation will occur in different regions of the sample for different frequencies. Thus, each time the frequency is changed, new hysteresis will be found for the first run after which this annealed configuration becomes stable. If  $A_s$  is increased too far, the changes become permanent since the motions now occur not only in the looser particle but also in the strong backbones of the arches.

If we scan frequency at a very low amplitude, we find a curve with many sharp features as was shown in Fig. 1(c). If we now increase the amplitude of the source, we find curves that are very similar to the initial one at low amplitude but with small frequency shifts. This is shown in Fig. 5(a) for the detector placed at a distance  $L_d = 4$  cm from the source. The curves are displaced vertically for clarity. As the source amplitude increases, we find a shift of the frequency of each feature to lower frequency. We also see that some features decrease in intensity as  $A_s$  increases, such as the feature at  $\nu = 4150$  Hz. Other features remain approximately independent of amplitude while others have been observed to increase in strength as  $A_s$  increases. We can measure the magnitude of the fre-

quency shift,  $\Delta\nu$ , as a function of  $A_s$  for each of the features. In Fig. 5(b) we show the results, taken from several different runs, for features in different frequency bins ranging from  $\nu = 1.5$  to 9.5 kHz. All of the shifts are toward lower frequency. There is no clear trend of the magnitude of  $\Delta\nu$  with frequency. This is shown in Fig. 5(c) where we plot  $\Delta\nu$  at a value of  $A_s = 0.07$  g versus frequency  $\nu$ . If the sound waves were localized, with a localization length depending strongly on frequency, we might have expected a correlation of  $\Delta\nu$  with  $\nu$  as had been found in a simulation of localized phonons in glasses.<sup>10</sup> The failure to find such a correlation indicates that the localization length may not be strongly dependent on frequency in the regime that we have investigated.

Sound propagation in granular media behaves in a number of unexpected ways. Even the simple measurement of the velocity of sound indicates complex behavior. Depending on how we perform the measurement in the linear response regime (e.g., by time of flight or by a measurement of phase versus frequency) we find that the velocities can differ by a factor of 5. However, if we increase the amplitude of the source we can explore nonlinear effects. The onset of nonlinearity is close to where we first see hysteretic behavior setting in. The behavior

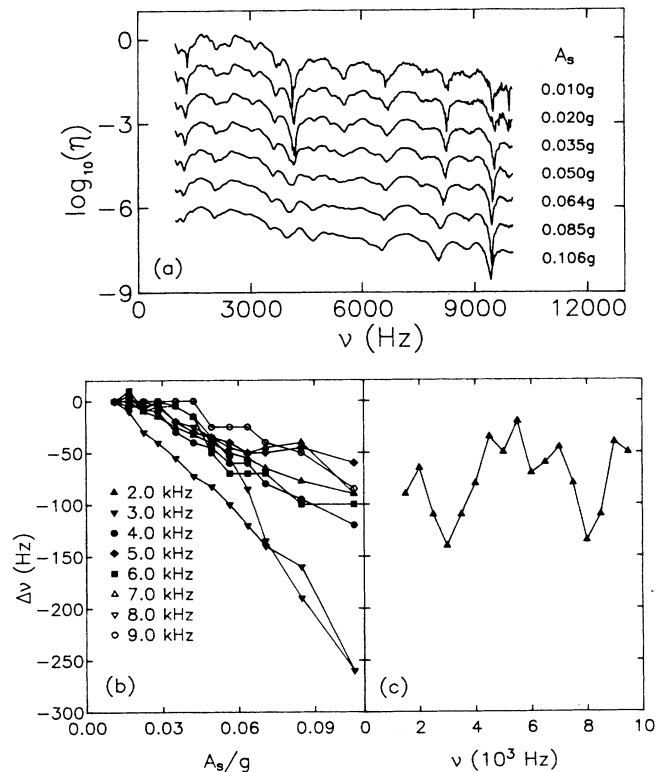


FIG. 5. (a) The frequency response function  $\eta(\nu)$  of the detector for seven different source amplitudes  $A_s$  as labeled in the figure. The detector is placed 4 cm away from the source. (b) The frequency shift  $\Delta\nu$  vs source amplitude  $A_s$  for eight frequency bins as labeled in the figure. (c) The frequency shift  $\Delta\nu$  vs frequency  $\nu$  at a source amplitude  $A_s = 0.07$  g.

of this hysteresis is consistent with an interpretation in terms of force chains that carry the sound. Minute rearrangements of the beads and their contacts can account both for the hysteresis and for the noise in the transmission of sound observed in our previous studies. As we increase the source amplitude, we also observe small frequency shifts in the features in the transmission spectra. In principle, these frequency shifts could have indicated the presence of localized vibrational modes with different localization lengths as a function of frequency. However, our data indicate that the magnitude of the shifts do not

strongly depend on frequency. We are presently extending our studies of the spatial extent of the modes by using the extreme dependence of the signal to small temperature fluctuations.

We would like to thank H. Jaeger, D. Johnson, J. Knight, M. Leibig, D. Sornette, C. Tang, D. Weitz, and T. Witten for stimulating discussions on various aspects of sound propagation in granular media. This work was supported by NSF Grant Nos. DMR-MRL 88-19860 and DMR 91-11733.

<sup>1</sup>See for example, H. M. Jaeger and S. R. Nagel, *Science* **255**, 1523 (1992), and references therein.

<sup>2</sup>C.-h. Liu and S. R. Nagel, *Phys. Rev. Lett.* **68**, 2301 (1992).

<sup>3</sup>In our previous paper (Ref. 2) we had quoted a value of 2.2 for the exponent. We are no longer convinced that the exponent is different from 2.0.

<sup>4</sup>M. Leibig (unpublished) has simulated some of these results.

<sup>5</sup>S. Feng and D. Sornette (unpublished).

<sup>6</sup>S. Washburn and R. Webb, *Adv. Phys.* **35**, 375 (1986); P. A. Lee and A. D. Stone, *Phys. Rev. Lett.* **55**, 1622 (1985); B. L. Al'tshuler, *Pis'ma Zh. Eksp. Teor. Fiz.* **41**, 530 (1985) [*JETP Lett.* **41**, 648 (1985)].

<sup>7</sup>D. J. Pine, D. A. Weitz, P. M. Chaikin, and E. Herbolzheimer, *Phys. Rev. Lett.* **60**, 1134 (1988); G. Maret and P. E. Wolf, *Z. Phys. B* **65**, 409 (1987).

<sup>8</sup>T. Travers, M. Ammi, D. Bideau, A. Gervois, J. C. Messenger, and J. P. Troadec, *Europhys. Lett.* **4**, 329 (1987), and references therein.

<sup>9</sup>This is the solution in 3 dimensions to the equation  $\partial R / \partial t = D \nabla^2 R$  with the boundary condition that  $R(t=0, r) = \delta(r)$ . For  $d$ -dimensional diffusion:  $R(\tau, r) = (4\pi D \tau)^{-d/2} \exp(-r^2/4D\tau)$ .

<sup>10</sup>S. R. Nagel, G. S. Grest, and A. Rahman, *Phys. Rev. Lett.* **53**, 368 (1984).